Twisting the Phenyls in Aryl Diphosphenes (Ar−P═P−Ar). Significant Impact upon Lowest Energy Excited States

Huo-Lei Peng,[†] John L. Payton, John D. Protasiewicz, and M. C. Simpson*[,‡]

Department of Chemistry and the Center for Chemical Dynamics, Case Western Reserve University, Cleveland, Ohio

Received: November 18, 2008; Revised Manuscript Received: April 9, 2009

Aryl diphosphenes (Ar−P═P−Ar) possess features that may make them useful in photonic devices, including the possibility for photochemical *E*−*Z* isomerization. Development of good models guided by computations is hampered by poor correspondence between predicted and experimental UV/vis absorption spectra. A hypothesis that the phenyl twist angle (i.e., PPCC torsion) accounts for this discrepancy is explored, with positive findings. DFT and TDDFT (B3LYP) were applied to the phenyl−P═P−phenyl (Ph−P═P−Ph) model compound over a range of phenyl twist angles, and to the Ph−P═P−Ph cores of two crystallographically characterized diphosphenes: bis-(2,4,6-*t*Bu$_3$C$_6$H$_2$)-diphosphene (Mes*−P═P−Mes*) and bis-(2,6-Mes$_2$C$_6$H$_3$)-diphosphene (Dmp−P═P−Dmp). A shallow PES is observed for the model diphosphene: the full range of phenyl twist angles is accessible for under 5 kcal/mol. The Kohn−Sham orbitals (KS-MOs) exhibit stabilization and mixing of the two highest energy frontier orbitals: the n_+ and π localized primarily on the −P═P− unit. A simple, single-configuration model based upon this symmetry-breaking is shown to be consistent with the major features of the measured UV/vis spectra of several diphosphenes. Detailed evaluation of singlet excitations, transition energies and oscillator strengths with TDDFT showed that the lowest energy transition ($S_1 \leftarrow S_0$) does not always correspond to the LUMO ← HOMO configuration. Coupling between the phenyl rings and central −P═P− destabilizes the $\pi-\pi^*$ dominated state. Hence, the S_1 is always $n_+-\pi^*$ in nature, even with a π-type HOMO. This coupling of the ring and −P═P− π systems engenders complexity in the UV/vis absorption region, and may be the origin of the variety of photobehaviors observed in diphosphenes.

Introduction

Since 1981, when Yoshifuji reported the first stable diphosphene (Mes*−P═P−Mes*),[1] a great many compounds with multiple bonds between heavy main group atoms have been described. Exploration of the synthesis, structures, coordination chemistry and reactivity of diphosphenes and related compounds is relatively advanced.[2−8] Less thoroughly investigated is the potential of diphosphenes for use as photoactive elements that is conferred upon them by their relationship to their chemical cousins azobenzene and stilbene.

The capability of photoactive molecules to impart functionality to materials has expanded greatly over the past 30 years or so. Molecular switches, memory elements, capacitors, sensors, modulators of liquid crystal optical properties and other photon-driven activities have been explored with success.[9−15] The patent literature abounds with hundreds of photoisomerization-based ideas, from portable body warmers[16] to solar energy collectors and storage elements.[17] Development of these technologies is still in the discovery phase, however, and diphosphenes (−P═P−) offer promising properties that are complementary to, or perhaps even superior to, those of their (−C═C−) and (−N═N−) counterparts.[18−23]

A natural first step toward exploring this promise is the computational characterization of diphosphene electronic excited states. Several computational studies have been reported (*vide infra)*, but have not revealed a consistent picture. In particular, the energetic ordering of the occupied frontier orbitals varies, and does not always reflect the experimental UV/vis absorption spectra. Careful examination of these published reports suggested to us that a deeper understanding of the impact of the phenyl twist angle (τ_1 and τ_2, Figure 1) upon the electronic behavior in diphosphenes might shed light on these issues and

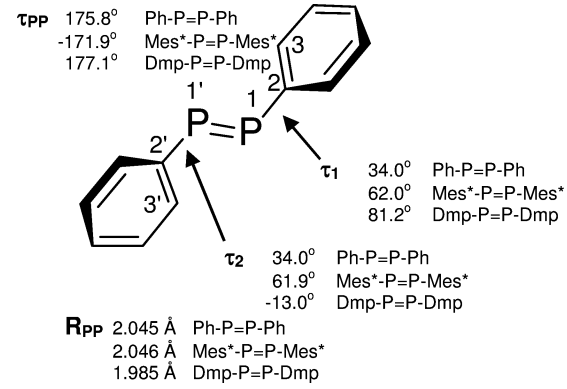

Figure 1. Important geometric parameters of *trans*-diphenyl diphosphene (Ph−P═P−Ph) optimized at the B3LYP/6-311+G(2df,2p) level (Table S2 in the Supporting Information). Comparisons to the crystal structures of Mes*−P═P−Mes* (ref 24) and Dmp−P═P−Dmp (ref 25) are provided as well. τ_1 (torsion angle 3−2−1−1′) and τ_2 (torsion angle 3′−2′−1′−1) are the phenyl twist angles relative to the −P═P− core unit, that is itself nearly planar (τ_{PP} = torsion angle 2′−1′−1−2). R_{pp} is the P═P bond length. For comparison to results from optimization at the B3LYP/6-31+G(d,p), see the Supporting Information.

* Corresponding author.
[†] Current address: Department of Chemistry, The Ohio State University, Columbus, Ohio.
[‡] Current address: Departments of Chemistry and Physics and The Dan Walls Centre for Pure and Applied Optics, The University of Auckland, Auckland, New Zealand.

10.1021/jp810119k CCC: $40.75
Published on Web 06/04/2009

foster further development of a useful framework within which to interpret ongoing and future photochemical and photophysical research.

Here, we report upon a thorough examination of the impact of varying phenyl-twist angles on diphosphene ground and excited states using DFT and TDDFT upon the bis-phenyl-diphosphene model compound (Ph−P═P−Ph; Figure 1). Constrained geometry optimizations were used to survey the Kohn−Sham molecular orbital (KS-MO) densities and energies versus phenyl twist angles. The potential energy surface (PES) along these degrees of freedom was probed as well, to determine the ease with which diphosphenes might undergo such distortions. The central Ph−P═P−Ph cores of the crystal structures of bis-(2,4,6-tBu$_3$(C$_6$H$_2$))-diphosphene (Mes*−P═P−Mes*)[1,24] and bis-(2,6-Mes$_2$C$_6$H$_3$)-diphosphene (Dmp−P═P−Dmp)[25] were treated as well, to ground the studies in experimental behavior.

UV/vis absorption spectra provide experimental access to electronic excited states and their energies, and insight into the participation of molecular orbitals in these photoactive states. Computational findings were therefore compared to the positions and relative intensities of the $S_1 \leftarrow S_0$ and $S_2 \leftarrow S_0$ transitions of several diphosphenes. A simple, frontier orbital model for diphosphene photobehavior was developed, and its limitations were explored. The model employs a pair of single excitations, localized mainly to the phosphorus−phosphorus unit. Such orbital-based models can have considerable value by enabling predictions of electronic absorption energies and relative intensities based upon relatively simple structural ideas.

While this simple model is consistent with many experimental findings, it has significant shortcomings. TDDFT demonstrates that the phenyl rings participate actively in modulating the UV/vis transitions, sometimes beyond what could reasonably be termed a perturbation. In fact, diphosphenes exhibit a relatively uncommon effect: the order and character of the HOMO and HOMO−1 do not translate with fidelity into the dominant descriptions of S_1 and S_2, respectively. Results are interpreted in terms of the impact of phenyl twisting upon diphosphene photochemistry and photophysics.

Computational Details

All computations were performed using Gaussian03[26] on a PC or high-performance computing (4 processors) platform. Full and constrained geometry optimizations were carried out using the B3LYP hybrid functional.[27−29] The 6-31G(d,p) basis[30] was utilized to calculate the potential energy surface of Ph−P═P−Ph along the τ_1 and τ_2 coordinates. A diffuse function was added (6-31+G(d,p)) for geometry optimizations at a few selected points along the diagonal $\tau_1 = \tau_2$. This level of theory was chosen as a reasonable balance between computational expense and accuracy. Calculations with a larger, more flexible basis set (6-311+G(2df,2p)) and tight optimization convergence limits showed only small (<10%) differences in both the ground and excited state findings. Results from the larger basis set are reported here, where available; a detailed comparison with the 6-31+G(d,p) basis set findings is provided in the Supporting Information.

This study focuses upon ground state structures and energies and vertical transitions to lower-lying excited states, with no chemical reactivity (i.e., bond breaking or forming), no intermolecular interactions, and no involvement of transition metals. Hence the B3LYP hybrid functional, by far the most widely used functional over the last several years,[31] is appropriate and this level of theory performs well for these target outcomes in main-group chemical systems of similar sizes and complexity.[31−33] Further, the B3LYP functional and a moderate basis set is generally sufficient for obtaining reliable TDDFT results, as long as the excitations remain well below the ionization threshold, as is the case here.[34] Finally, this report also treats the KS-MOs on par with *ab initio* molecular orbitals, as accurate reflections of the electronic behavior of the system.[35]

At the minimum energy structure determined by an unconstrained geometry optimization, no negative vibrational frequencies were found. When symmetry was enabled, C_2 symmetry was found for all structures except the $\tau_1 = \tau_2 = 0°$ point, which was found to be in the C_{2h} point group. Parallel computations without symmetry constraints confirmed that the results were not distorted by exploiting the symmetry of the system. Pruned Ph−P═P−Ph versions of the experimental crystal structures of Dmp−P═P−Dmp[25,36] and Mes*−P═P−Mes*[24] were created by removing the ligand atoms down to the base phenyl rings and substituting hydrogens. The C−H bonds were allowed to relax to minimum energy positions, and the ground state KS-MOs and their energies were calculated at the B3LYP/6-31+G(d,p) level. Transition energies and excited states were calculated upon Ph−P═P−Ph geometries and upon the Mes*−P═P−Mes* and Dmp−P═P−Dmp core geometries using TDDFT/B3LYP/6-31G+(d,p)). The steric impact of the ligand bulk upon the phenyl twist barriers was estimated with a series of ground state calculations of bis-(2,6-tBu$_2$(C$_6$H$_2$)) diphosphene along the $\tau_1 = \tau_2$ diagonal of the PES. Molecular orbital images were generated by GaussView3.0 on a PC platform.[37] Fitting of KS-MO energies to $y = a + b\cos^2(\tau)$ was performed using Origin 7.5.

Results and Discussion

This study began with the geometry optimization of a model compound, Ph−P═P−Ph, at a relatively high level of density functional theory (B3LYP/6-31+G(d,p)). Many experimental diphosphenes attach phenyl-based bulky groups to the phosphorus atoms to kinetically stabilize the −P═P− double bond. Hence Ph−P═P−Ph was chosen to appropriately balance computational expense and authentic molecular features such as steric repulsions and π-interactions. The surprising result was that the order of the two highest energy occupied orbitals was not consistent with experiment, leading to inaccurate predictions of UV/vis absorption and photochemical behavior.

At the B3LYP/6-311+G(2df,2p) level of theory, the minimum energy structure of *trans*-Ph−P═P−Ph does not have planar C_{2h} symmetry, in contrast to the analogous *trans*-Ph−(H)C═C(H)−Ph and *trans*-Ph−N═N−Ph species. Although the central −P═P− unit is nearly planar ($\tau_{PP} = 175.8°$), the phenyl rings are twisted by 34° (Figure 1), presumably to relieve repulsions between the relatively large third-shell phosphorus lone pairs and phenyl *ortho*-hydrogens. These steric repulsions are further exacerbated by the small C−P═P angle (102.3°), that arises from the less effective sp^2 hybridization that is observed in heavier main group systems.[5,38]

A very recent study using a complete active space self-consistent field (CASSCF) approach is in agreement with these findings as well.[39] The minimum energy geometry on S_0 was found to have a phenyl torsion angle of 30.3°, quite similar to the B3LYP/6-311+G(2df,2p) and B3LYP/6-31+G(d,p) results reported here.[40]

In experimentally characterized diphosphenes, the use of bulky groups to protect the reactive −P═P− bond leads to a wide range of phenyl twist angles (Table 2). This observation suggests that phenyl twisting provides an energetically thrifty path for the molecule to relieve steric stresses.

TABLE 1: Computed and Experimental Electronic Transition Energies and Strengths of Mes*−P═P−Mes* and Dmp−P═P−Dmp[a]

	Mes*−P═P−Mes*				Dmp−P═P−Dmp			
	calc[b]		expt[c]		calc[b]		expt[c]	
	λ	f	λ	ε	λ	f	λ	ε
$n_+ \rightarrow \pi^*$	488	0.0345	460	1360	447	0.0006	456	365
$\pi \rightarrow \pi^*$	346	0.0630	340	7690	347	0.177	372	6190

[a] λ in nanometers; f in atomic units; ε in M^{-1} cm^{-1}. [b] B3LYP/6-31+G(d,p) single point calculations of Ph−P═P−Ph core of the crystal structures, as described in the text. [c] Mes*−P═P−Mes* in CH_2Cl_2; Dmp−P═P−Dmp in heptane.

Energetic Cost of Phenyl Twisting. To evaluate the energetic expense of phenyl twisting, the ground state PES (361 points) was computed along τ_1 and τ_2 (B3LYP/6-31G(d,p)) (Figure 2). The shallow surface illustrates the ease with which the system can distort along these coordinates to accommodate substituents. A significantly larger, more flexible basis set (6-311+G(2df,2p) basis set was employed to examine the diagonal ($\tau_1 = \tau_2$) of the PES with higher fidelity. The energy differences between the minimum at 34° and the maxima at 0° and 90° are 0.0246 eV (0.567 kcal mol^{-1}) and 0.162 eV (3.74 kcal mol^{-1}), respectively. This energy barrier at $\tau = 90°$ is slightly greater than that found by Y. Amatatsu using a multireference *ab initio* method.[39,41] The entire range of phenyl twist angles is available for less than 4 kcal mol^{-1}, and structures from 0° to about 50° are accessible at room temperature (within ~250 cm^{-1} of the minimum).[37]

This low barrier to phenyl twisting in Ph−P═P−Ph is significantly smaller than what is observed for azobenzene and stilbene. At the same level of theory, these compounds exhibit planar minimum energy structures and larger barriers to phenyl rotation of 0.479 eV (11.0 kcal mol^{-1}) and 0.381 eV (8.79 kcal mol^{-1}), respectively. Evidently, π-delocalization is weaker in diphosphene than in either of its lighter element cousins. That there is some conjugation in the Ph−P═P−Ph system is apparent in the increase in the P−C bond length from 1.831 to 1.847 Å as the phenyl rings are twisted from 0° to 90°. Experimental evidence for π-delocalization also can be seen in an elegant study by Petsana and Power of a set of diarylboryl-substituted diphosphanes.[42,43] In these molecules, the P-atoms are bonded through only the σ-component of the double bond (i.e., the sp^2 hybrid P−P σ-bond in the absence of P═P π-bonding) and the P−C bonds are a few hundredths of an angstrom longer than the corresponding bonds in Mes*−P═P−Mes* and Dmp−P═P−Dmp. The shorter P−C bonds in the latter molecules support the presence of π-delocalization across the Ph−P═P−Ph architecture.

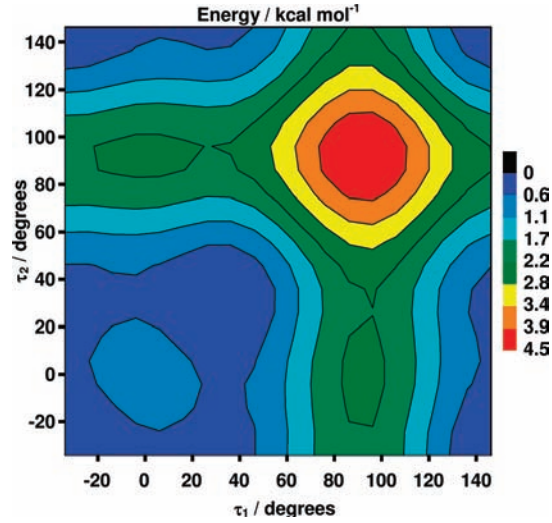

Figure 2. Ground state potential energy surface along the τ_1 and τ_2 phenyl twisting coordinates. B3LYP/6-31G(d,p) level for Ph−P═P−Ph. The energy was calculated every 10° from −34° to 146° (361 points). All other geometric parameters were allowed to optimize. Energy is in kcal/mol, and is relative to the minimum.

In aryl-diphosphenes, π-delocalization appears strong enough to shorten P−ligand bonds and create a moderate barrier to phenyl ring twisting, but not strong enough to induce coplanarity among the phenyl rings and the central C−P═P−C unit. This begs the question: why is conjugation across the molecule less effective in diphosphene than in stilbene and azobenzene? Probably the most important factor is the relative sizes of the atomic p-orbitals involved. The $\langle r \rangle$ for the phosphorus 3p orbital is about 40−50% larger than that for the carbon 2p orbital,[38] significantly limiting the magnitude of their overlap integral. The reduced π-overlap is probably compounded by the inefficient sp^2 hybridization at the phosphorus. In general, hybridization is less important for larger main group elements than for cognate lighter systems.[2,5,38,44] In diphosphenes, this is reflected in larger s-character for the lone-pair electrons and C−P═P bond angles that are closer to 90° than to 120°. The impact of the relatively poor π-overlap can be seen in estimates of σ and π contributions to homonuclear and heteronuclear double bonds among C, N, and P. The π-increment[45] for the CC bond is ~70 kcal/mol, and is similar in magnitude to that for NC (~65−86 kcal/mol); both are significantly larger than for PC (~45−50 kcal/mol).[38,46,47] By extension, delocalized π-bonding across the Ar−P═P−Ar molecule might be relatively inefficient. In combination with the large extent of the phosphorus lone pairs and smaller ligand−E═E angle, this weaker conjugation induces diphenyl diphosphene to inhabit a more

TABLE 2: Electronic Transition Energies and Strengths of Some Real Diphosphenes[a]

		UV/vis absorption			
compound[b]	τ_1, τ_2	$\pi-\pi^*$	$n_+-\pi^*$	intensity ratio	ref
Tbt−P═P−Tbt	52.8, 60.0	405 (13000)	530 (2000)	0.15	78
Dmop−P═P−Dmop[c]	61.3, 58.6	346 (5620) 347 (5500)	477 (1320) 478 (1260)	0.23, 0.23	79, 80
Mes*−P═P−Mes*	61.5	340 (7690)	460 (1360)	0.18	1
Dmp−P═P−Dmp	81.2, 13.0	372 (6190)	456 (365)	0.059	25
Bbt−P═P−Bbt	86.2, 28.4	428 (12000)	532 (1000)	0.083	78
Dcp−P═P−Dcp	88.7	352 (8551)	448 (626)	0.073	81
Btfmp−P═P−Btfmp	91.8	277 (11640)	394 (197)	0.017	82, 83

[a] τ_1 and τ_2 phenyl torsion angles defined in Figure 1, in degrees; λ in nanometers; ε in M^{-1} cm^{-1}. [b] Tbt = 2,4,6-tris[bis(trimethylsilyl)-methyl]phenyl; Dmop = 2,6-di-*tert*-butyl-4-methoxyphenyl; Mes* = 2,4,6-tri-*tert*-butylphenyl; Bbt = 2,6-bis[bis(trimethylsilyl)-methyl]-4-[tris(trimethylsilyl)methyl]phenyl; Dcp = 2,6-(2,6-$Cl_2C_6H_3$)C_6H_3; Btfmp = 2,6-bis(trifluoromethyl)phenyl. [c] CH_2Cl_2 (upper), hexane (lower).

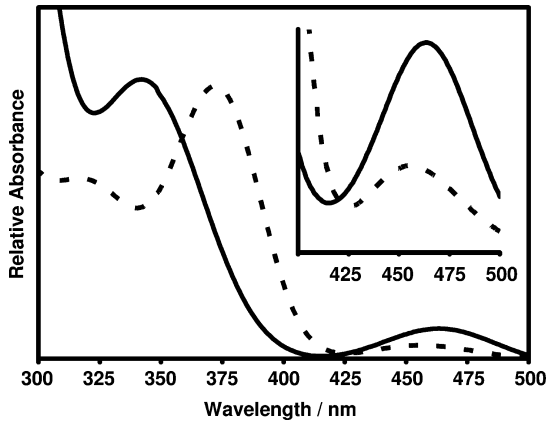

Figure 3. UV/vis absorption spectra of Mes*−P═P−Mes* (solid line; $\varepsilon_{340} = 7.69 \times 10^3$ M^{-1} cm^{-1} and $\varepsilon_{460} = 1.36 \times 10^3$ M^{-1} cm^{-1} in CH_2Cl_2) and Dmp−P═P−Dmp (dotted line; $\varepsilon_{372} = 6.19 \times 10^3$ M^{-1} cm^{-1} and $\varepsilon_{456} = 365$ M^{-1} cm^{-1} in heptane).

twisted region of the PES than do azobenzene and stilbene. The bulky ligands required to stabilize diphosphenes magnifies this tendency by increasing the barrier to phenyl rotation at $\tau_1 = \tau_2 = 0°$ (*vide infra*).

Phenyl Twists, Frontier Orbitals, and the UV/Vis Spectrum. A Simple Model. The shallow PES along the phenyl twists is noteworthy because of the marked effect this distortion has upon the frontier molecular orbitals. These can be sensitive controllers of the UV/vis spectrum and photoreactivity. Diphosphenes typically exhibit two major UV/vis absorptions (Figure 3), both assigned primarily to the P═P group. An intense (ε_{max} ~10,000 cm^{-1} M^{-1}) transition in the 330−350 nm region is attributed to a $\pi-\pi^*$ excitation; a much less intense (ε_{max} ~1,000 cm^{-1} M^{-1}) band at about 460 nm is assigned to the symmetry-forbidden $n_+-\pi^*$ transition.

As mentioned above, the frontier orbitals of the calculated minimum energy *trans*-Ph−P═P−Ph ($\tau_1 = \tau_2 = 34°$) are in conflict with experimental observations: the HOMO is calculated to be largely π, the HOMO−1 is largely n_+ and the LUMO is antibonding π^* (Figure 4). These results predict that the $\pi-\pi^*$ and $n_+-\pi^*$ UV/vis transitions should be reversed from the observed order. Further, these results conflict with previous DFT calculations on the crystal structure of Mes*−P═P−Mes*[24] and on Ph−P═P−Ph with the phenyls fixed to the twist angle ($\tau_1 = \tau_2 = 64°$) near that of the Mes*−P═P−Mes* crystal structure, both of which assigned the HOMO to be an n_+ orbital.[48,49]

Several previous computational studies, mostly on H−P═P−H, also predicted that the HOMO should be a π orbital. These included several Hartree−Fock self-consistent field (HF-SCF) studies[50−52] and one that employed CASSCF.[53] Others indicated that the HOMO was an n_+ orbital,[54−57] and used this information to definitively assign the Mes*−P═P−Mes* photoelectron spectrum, with the n_+ as the HOMO by the Koopmans theorem. Allen and co-workers resolved the issue for H−P═P−H in an elegant and thorough computational study, and determined that correlation is required to obtain the appropriate orbital ordering.[58] Later, B3LYP/6-311G(d,p) calculations on H−P═P−H also found the HOMO to be n_+.[48] In light of all of these findings, it was concluded that the level of theoretical treatment employed in our B3LYP studies on Ph−P═P−Ph should be sufficient to accurately predict the order of frontier orbitals, though they are energetically close. A structural origin for the discrepancy was proposed, in line with a suggestion by Miqueau et al.[48]

To test this hypothesis, the energies and orbitals were calculated for Ph−P═P−Ph as a function of phenyl twist angle. The KS-MOs for Ph−P═P−Ph as they are systematically distorted along the $\tau_1 = \tau_2$ diagonal of the PES are shown in Figure 4 (B3LYP/6-31+G(d,p)). For the constrained planar Ph−P═P−Ph, the two highest occupied orbitals are very clearly π (HOMO) and n_+ (HOMO−1). As expected from the C_{2h} symmetry, these π (a_u) and n_+ (a_g) orbitals are pure and orthogonal. Twisting about the phenyl rings, however, reduces them to the same symmetry (a) and mixing occurs. Figure 4 (upper panel) shows this progressive, structurally induced orbital transformation.

The energies of the occupied frontier orbitals depend upon the phenyl twist angle (Figure 5; B3LYP/6-311+G(2df,2p)). The HOMO and HOMO−1 are separated by 0.56 eV in the planar molecule, in good agreement with Allen et al.,[58] and are stabilized roughly in parallel across the range of $\tau_1 = \tau_2$ angles. The stabilization fits a $\cos^2 \tau$ ($\tau = \tau_1 = \tau_2$) dependence ($r^2 > 0.99$), indicating that $\pi-\pi$ overlap between the ring and central −P═P− is the prevailing influencing factor.

Examination of the end points ($\tau = 0°$ and $\tau = 90°$) for the HOMO and HOMO−1 in Figure 5 shows a net stabilization (~1 eV) of the π-character, and a significantly smaller destabilization of n_+. In contrast, the π^* LUMO shape and energy remain largely constant with phenyl twist angle; the energy changes by less than 0.12 eV over the entire phenyl twist range (Table S2 in the Supporting Information). Given the nodes between the −P═P− and the phenyl rings in this orbital, this insensitivity is entirely consistent with a π-overlap dependence.

It is worthwhile to consider a simple model in which the HOMO, HOMO−1, and π^* LUMO determine the major features of the UV/vis spectroscopic and photochemical behavior. Such frontier orbital models have shown excellent results in many organic photoactive systems, particularly by providing significant qualitative, physical insight into the photophysics and photochemical reactivity. First, we ascribe the dominant phenyl twist impact to the ground state, and mix the two highest-energy, occupied, frontier orbitals according to $\cos^2(\tau)$. Then, the UV/vis absorption spectrum is described by single electronic configurations: S_1 thus corresponds cleanly to LUMO ← HOMO and S_2 corresponds to LUMO ← HOMO−1. Several qualitative predictions can be made with this model:

1. Both $S_1 \leftarrow S_0$ and $S_2 \leftarrow S_0$ transitions will appear in the UV/vis absorption spectrum, except when $\tau_1 = \tau_2 = 0°$ or 90°. For these geometries, one transition would correspond to pure $\pi^* \leftarrow n_+$ and be symmetry forbidden. At all other angles, both excitations will have some $\pi^* \leftarrow \pi$ character, the magnitude of which would be reflected in the bands' relative intensities. The intensities should be most similar when $\tau_1 = \tau_2 = 45°$.
2. The order of the UV/vis absorption bands will depend upon the phenyl twist angle. For $\tau_1 = \tau_2 > 45°$, the more intense band will arise at higher energy with a less intense one to the red; for $\tau_1 = \tau_2 < 45°$, the more intense transition will occur at lower energy.
3. As the phenyl twist increases, the HOMO and HOMO−1 are stabilized while the LUMO energy is unaffected; hence both bands should blue-shift as the phenyl twist increases.

Comparisons to Experimental Data. The first two predictions from the simple model above are largely borne out in experimental findings. The HOMO and HOMO−1 derived from single-point calculations of the core structures from crystal data of the diphosphenes Mes*−P═P−Mes* and Dmp−P═P−Dmp are shown in Figure 4 (lower panel). Both show a HOMO dominated by n_+ character. The experimental $S_2 \leftarrow S_0$ transition of Mes*−P═P−Mes* is at 340 nm ($\varepsilon_{340} = 7.69 \times 10^3$ M^{-1}

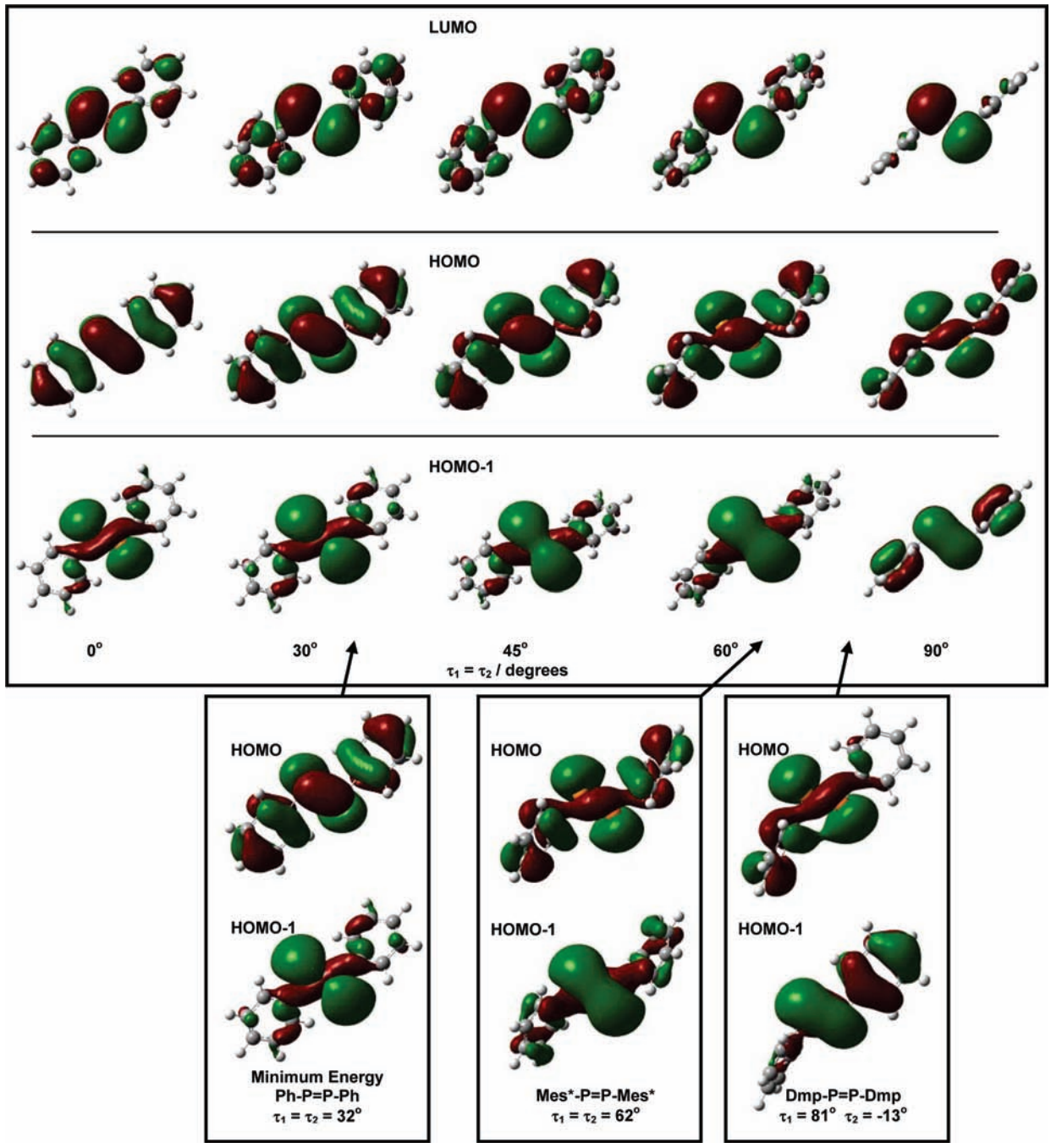

Figure 4. Upper panel: Frontier Kohn−Sham orbitals from geometry optimizations constrained along the $\tau_1 = \tau_2$ diagonal of the ground state potential energy surface. Lower panel: Highest occupied Kohn−Sham orbitals from (left to right) unconstrained geometry optimized Ph−P═P−Ph, Ph−P═P−Ph core of the crystal structure of Mes*−P═P−Mes*, and Ph−P═P−Ph core of the crystal structure of Dmp−P═P−Dmp. All calculations performed at the B3LYP/6-31+G(d,p) level.

cm^{-1}), and that of Dmp−P═P−Dmp is at 372 nm ($\varepsilon_{372} = 6.19 \times 10^3\ M^{-1}\ cm^{-1}$) (Table 1). The weaker band ($S_1 \leftarrow S_0$) appears at lower energy for both molecules, hence the order of the UV/vis absorption transitions is qualitatively consistent with the single configuration model.

The relative intensities of the bands support the single configuration model as well. Mes*−P═P−Mes*, with $\tau_1 = \tau_2 = 62°$, is closer to the fully mixed 45° model conformation than is Dmp−P═P−Dmp. Hence the relative intensity of the $n_+ - \pi^*$ band to the $\pi - \pi^*$ should be larger for Mes*−P═P−Mes*. This is, in fact, observed: the measured ratio of band intensities $\varepsilon_{(n_+ - \pi^*)}/\varepsilon_{(\pi - \pi^*)}$ is 0.18 for Mes*−P═P−Mes* and 0.059 for Dmp−P═P−Dmp.

Table 2 indicates that this simple model qualitatively captures the UV/vis absorption behavior of other diphosphenes as well. All of these diphosphenes exhibit at least one $\tau_1 = \tau_2$ greater than 45°, and the lower energy absorption is less intense for all of them. Further, when the phenyl twists are in the 50−65° range, the ($S_1 \leftarrow S_0$):($S_2 \leftarrow S_0$) relative intensity ratio is 0.15−0.25. With at least one $\tau > 80°$, the ratio decreases substantially to 0.02−0.08, as predicted.

The phenyl twist angles of stable diphosphenes tend to be significantly larger than the 34° equilibrium value determined for diphenyl diphosphene, a molecule that has never been isolated or observed in experiments. B3LYP/6-31+G(d,p) calculations upon bis-(2,6-tBu$_2$(C$_6$H$_2$)) diphosphene, a model

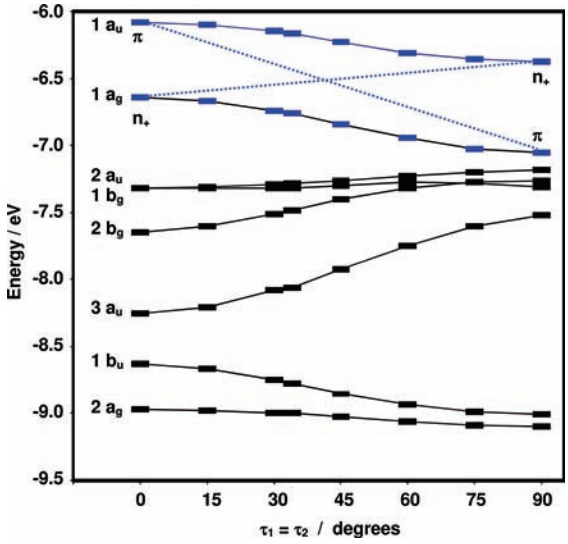

Figure 5. Energies of the eight highest energy occupied Kohn−Sham molecular orbitals (B3LYP/6-311+G(2df,2p)) of Ph−P═P−Ph at a series of $\tau_1 = \tau_2$ phenyl twist angles. Symmetry designations derive from the constrained planar conformation ($\tau_1 = \tau_2 = 0°$). The two frontier orbitals in the simple model, single-configuration model are in blue. For comparison to results from optimization at the B3LYP/6-31+G(d,p), see the Supporting Information.

for Mes*−P═P−Mes*, along the $\tau_1 = \tau_2$ diagonal of the PES produce a more distorted minimum energy structure at $\tau_1 = \tau_2 = 63.4°$, quite close to the experimental crystal structure value for Mes*−P═P−Mes* (Supporting Information). The barrier to phenyl rotation at 0° has increased significantly to 1.12 eV (25.9 kcal/mol). Thus, the steric crowding introduced by the bulky ligands significantly narrows the range of phenyl twist angles available to the molecule at room temperature, to between about 60° and 70° (within ~250 cm^{-1} of the minimum). Hence the molecule does exploit the soft PES of the phenyl twist degree of freedom inherent in the Ph−P═P−Ph to accommodate bulky ligands, and the greatly increased barrier at $\tau_1 = \tau_2 = 0°$ appears to constrain the molecule to a relatively narrow range of the larger phenyl twist angles. This finding and the agreement between the calculated and experimental values also suggest that crystal packing forces may have a relatively minor impact upon the phenyl twist angle, and suggest that the phenyl twist angles adopted by diphosphenes in room temperature solutions may be similar to those observed in crystal structures, in general.

The results thus far indicate that Ph−P═P═Ph is a good model for capturing important diphosphene photobehavior, and the B3LYP/6-31+G(d,p) level of theory is appropriate for this system. The phenyl twist indeed appears to exert significant influence over the two highest energy frontier orbitals, and thereby upon the diphosphene UV/vis absorption spectrum. Electronic transitions dominated by single configurations thus appear to explain the major features of diphosphene UV/vis spectroscopy, once the impact of the phenyl twist upon the orbitals is taken into account, though the model has some limitations (*vide infra*).

Phenyl Twist and Excited States. The Picture Is More Complex. The third prediction from the single-configuration model—that both $S_2 \leftarrow S_0$ and $S_1 \leftarrow S_0$ should blue shift with increasing phenyl twist angle—is not borne out by experimental findings. Limitations of the single-configuration model can be illustrated by comparing Tbt−P═P−Tbt and Dmop−P═P−Dmop.[59] These two molecules have similar phenyl twist angles, but their UV/vis absorption bands differ by more than 50 nm. Evidently, and not surprisingly, the absolute band energies reflect interactions with the protecting groups beyond the influence of the phenyl twist upon the three frontier orbitals in the simple model.

To explore the UV/vis transition energies and intensities in more detail, TDDFT (B3LYP/6-31+G(d,p)) calculations were performed upon the two truncated diphosphene model structures discussed above (Table 1). For Mes*−P═P−Mes*, less than 10 nm separates the TDDFT calculated and observed wavelengths for the higher energy, higher intensity transition. The $n_+-\pi^*$ is calculated at somewhat too long a wavelength at 488 nm, but the agreement with experiment is still good. The Dmp−P═P−Dmp lower energy band is quite well reproduced, though the ($S_2 \leftarrow S_0$) is slightly less well so. The oscillator strengths emulate the experimental results as well, albeit in an exaggerated fashion.

The discrepancies between experiment and computation may be partly due to the electronic influence of the extended groups that are absent from the calculations. Symmetry breaking may also play a role for Dmp−P═P−Dmp. However, the TDDFT descriptions of the S_1 and S_2 states point clearly to the participation of other electronic excitations in the observed UV/vis transitions, especially those involving the phenyl ring π-systems.

For both the Dmp−P═P−Dmp and Mes*−P═P−Mes* core model structures, the S_1 state contains significant contributions from LUMO ← HOMO and LUMO ← HOMO−1 excitations, though the former has a 4−5-fold larger coefficient. The higher energy, more intense transition is more complex. While the LUMO ← HOMO−1 is the largest contributor to the S_2 state, three other excitations also are significant; these are all excitations from ring π-orbitals to the LUMO. Also, LUMO ← HOMO−1 participates in other states that exhibit appreciable oscillator strengths. This latter detail could be the origin of the exaggerated relative intensity predictions: the measured $\pi-\pi^*$ transition is likely to be a composite of several bands of varying oscillator strengths.

The limitations of the simple model were explored further by applying TDDFT/B3LYP/6-311+G(2df,2p) across the entire range (0° to 90°) of phenyl twist angles (see Supporting Information for TDDFT/B3LYP/6-31+G(d,p) results). The results indicate that although the single-configuration model is qualitatively consistent with experiment, it is overly simple. The ring π systems participate rather heavily in the "P═P" transitions, and in a τ-dependent manner, to tune the energies and transition moments of the excited states.

The most surprising finding was that the $n_+-\pi^*$ dominated transition is *always* the lower energy one, even when $\tau_1 = \tau_2 < 45°$, where the HOMO is clearly a π-type orbital. In fact, even at $\tau = 0°$, where the HOMO is clearly a π-type orbital, the S_1 state is quite unambiguously assigned to the ($n_+^1\pi^{*1}$) configuration, and S_2 to ($\pi^1\pi^{*1}$).[60]

Insight can be found by examining the occupied orbitals just *below* the HOMO and HOMO−1 (Figure 5).[61] At $\tau_1 = \tau_2 = 0°$, the π HOMO is $1a_u$ and the n_+ HOMO−1 is $1a_g$. Two other a_u orbitals lie within about 2 eV of $1a_u$. The $2a_u$ π-orbital resides wholly on the phenyls, while $3a_u$ has a large π-bonding contribution that spans the central part of the molecule. Phenyl twisting destabilizes $3a_u$, as expected by its electron density. The energies of these KS-MOs converge as the phenyl twist angle increases. By $\tau = 90°$, the HOMO is a relatively energetically isolated n_+ orbital, 0.7 eV above the HOMO−1. Next come 5 π orbitals within an energy range of 0.4 eV. Thus

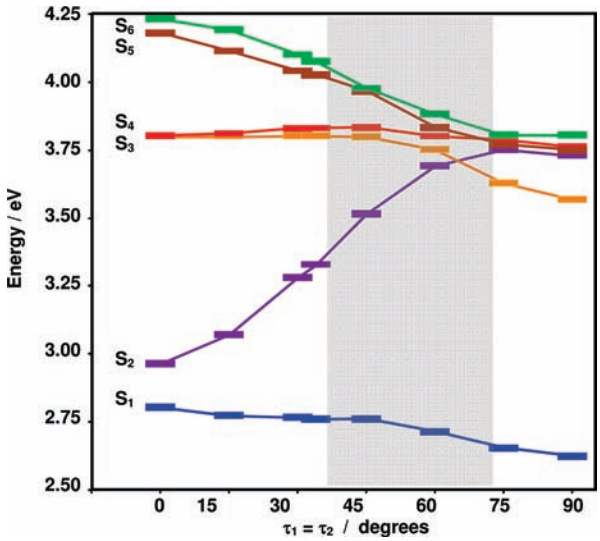

Figure 6. Energies of the six lowest energy singlet excited states (TDDFT/B3LYP/6-311+G(2df,2p)) of Ph−P═P−Ph at a series of $\tau_1 = \tau_2$ phenyl twist angles. Excited state designations relate to the constrained planar conformation ($\tau_1 = \tau_2 = 0°$). The states corresponding to transitions traditionally assigned to $n_+ - \pi^*$ (S_1) and $\pi - \pi^*$ (S_2) are in blue and violet, respectively. The gray area highlights the phenyl twist angles exhibited by many experimental diphosphenes. For comparison to results from optimization at the B3LYP/6-31+G(d,p), see the Supporting Information.

the extended π-system has the energy and symmetry properties favorable for participation in the $S_2 \leftarrow S_0$ transition.

The TDDFT results confirm that the most intense band in the UV/vis absorption spectrum is not isolated to the P═P unit: by $\tau_1 = \tau_2 = 30°$, contributions from electronic excitations involving ring and ring-P π-orbitals are significant, and mixing increases with τ. In fact, as the phenyl twist increases from 60° to 90° the transitions become so mixed it becomes challenging to assign them. At 75°, for example, four singlet states with nonzero oscillator strengths are clustered within 0.06 eV of one another (Figure 6). Thus the observed band assigned to the P═P $\pi - \pi^*$ excitation is relatively complex, with multiple contributions from the ring π-system that depend sensitively upon the phenyl twist angle.

In contrast, S_1 remains relatively uncomplicated throughout. It contains significant contributions from only configurations involving the HOMO, HOMO−1, and LUMO throughout the range of phenyl twist angles. Presumably, it remains the lowest energy state because the mixing of the higher energy configurations with the lowest energy ($\pi^1\pi^{*1}$) destabilizes S_2. However, further study is required to fully understand this observation.

As this manuscript was being finalized, a very relevant report of *ab initio* calculations upon the phenyl twisting degree of freedom in Ph−P═P−Ph was published.[39] In those studies, CASSCF was employed to optimize the geometries of the S_0 state along this coordinate, and second-order multireference Moller−Plesset perturbation theory (MRMP2) energies were calculated for S_0 and S_1 at these CASSCF geometries. Although the more intense transition to S_2 was not discussed in that paper, the major features of the *ab initio* results agree quite well with the TDDFT B3LYP/6-311+G(2df,2p) findings for the $S_1 \leftarrow S_0$ excitation.

A straightforward DFT analysis has revealed important subtlety in the electronic structure of diphosphenes in just the range of phenyl twist angles that are experimentally common: 45° − 90°. While the simple, single-configuration model provides useful qualitative insight, a more detailed treatment of the coupling between −P═P− and phenyl π systems may be needed to account for details in the interaction of diphosphenes with light.

Potential Impact upon Photochemistry. The shallow nature of the PES along the two-dimensional CCPP surface accounts for the broad structural diversity observed experimentally for these phenyl twist angles in diphosphenes. Concomitantly, the impact of the phenyl twist upon the energies and natures of the electronic excited states shown here may help explain the photochemical and photophysical diversity exhibited by diphosphenes.

Direct studies of diphosphene photobehavior are relatively limited, yet the richness they reveal is considerable. Consider the molecules most thoroughly discussed here: Dmp−P═P−Dmp and Mes*−P═P−Mes*. Excitation of Mes*−P═P−Mes* in the ultraviolet induces irreversible CH bond-insertion into the Mes* group, possible through a phosphinidene intermediate, to produce a phosphaindan product.[62,63] In contrast, Dmp−P═P−Dmp undergoes no *irreversible* photochemistry under similar conditions. Fluorescence is negligible for both at room temperature, consistent with very rapid excited state evolution. Femtosecond transient absorption confirms that the initial dynamics are sub-picosecond, however subsequent dynamics differs for the two systems.[64,65]

Photoisomerization from the *trans* to *cis* conformations, and back, is observed for several diphosphenes, including Mes*−P═P−Mes* under some conditions.[63,66−73] In some cases, the formation of a labile cyclotetraphosphane arising from the head-to-head dimerization of *cis*-diphosphenes is experimentally observed[66,74,75] or implied by the products formed.[69,73,76] In other photochemical experiments, evidence for a transient cyclotetraphosphane is sought but not found.[70,72] Photoinduced bond insertion of the phosphorus into ligand C−H or C−C bonds is also observed, perhaps through a phosphinidine intermediate.[62,63,69,70]

It is unlikely that the phenyl twist is the *sole* variable responsible for variety observed in the photobehavior of diphosphenes. There is ample evidence in the studies above for other influences by the bulky ligands, including electronic factors and proximity of C−C and C−H bonds to phosphorus atoms, and for temperature- and excitation wavelength-dependence in the above photoinduced reactions. However, the provocative initial computational findings reported here lead to a reasonable hypothesis that the phenyl twists may have an impact upon diphosphene photochemistry and photophysics, through moderation of the coupling between the phenyls and the central −P═P−. The flat PES may mean that diphosphenes in solution sample a broad range of the phenyl twist angles. The character of the photoexcited state(s) will affect the internal conversion and intersystem crossing events, excited state lifetimes, pathways, and product distributions. Recent reports of the importance of the phenyl ring states in critical aspects of azobenzene photochemistry provide further support for this idea.[77]

Clearly, these findings are just the first step in elucidating the structure−function relationships that drive the photodynamics of diphosphenes. Further exploration of the excited state potential surfaces, and interpretation of new femtosecond transient absorption findings are underway in our group. A more rigorous study of the rotation, inversion, and dissociation pathways along the ground and excited electronic states of diphosphenes using complete active space methods will be reported separately.

Summary

DFT and TDDFT have been applied to a model diphosphene to resolve a puzzling conflict in the 25-year diphosphene computational chemistry literature. The HOMO and HOMO−1 in this system are energetically close, and while the UV/vis spectrum of all diphosphenes synthesized thus far indicates that the n_+ orbital should be the HOMO, a number of computational treatments have found otherwise. Allen et al. definitively showed that effective correlation is needed to properly order the frontier occupied orbitals in HP═PH.[58] Here we report that there is a molecular structure effect operating as well, one that can affect experimental diphosphene behavior.

In arguably the most important class of diphosphenes, aryl−P═P−aryl, conjugation with phenylic substituents has a significant impact upon the occupied frontier orbitals. Although the π-delocalization across the molecule is relatively weak, the near-degeneracy of the two occupied frontier molecular orbitals leads to its significant consequences. As the π-overlap between the central −P═P− unit is "tuned" by twisting the phenyl ligands, the HOMO and HOMO−1 mix and are concomitantly stabilized, resulting in a net transformation of the HOMO from π to n_+ in character, and the HOMO−1 from n_+ to π. Nonetheless, even over the range of angles where the HOMO is clearly a π-orbital, the S_1 state equally clearly arises from a primarily ($n_+^1\pi^{*1}$) excitation. Coupling between the π-systems of the −P═P− and the phenyl rings stabilizes the ($\pi^1-\pi^{*1}$) state, in a phenyl twist dependent manner.

The energy barrier to phenyl twisting motion is quite small, and the diversity of phenyl twist angles observed experimentally indicates that many diphosphenes exploit the ease of distortion to relieve stress. As the search for new functional materials continues to intensify, understanding the photochemistry and photophysics of the heavier main group compounds becomes increasingly important. This study reveals very useful information that confirms and extends what is known about the bonding and spectroscopy of the promising diphosphene class of molecules, and helps to lay the groundwork for future studies.

Acknowledgment. We thank the NIH (MCS GM056816), the NSF (CHE-0518510 to M.C.S.; CHE-0202040 to J.D.P.) and the Provost's Opportunity Fund at CWRU (M.C.S.) for financial support. This research was also supported by an NSF ADVANCE Institutional Transformation Grant SBE-0245054, Academic Careers in Engineering and Science (ACES) at Case Western Reserve University (M.C.S.).

Supporting Information Available: References with more than 10 authors. Table S1: Selected geometric parameters and KS-MO energies for distorted Ph−P═P−Ph (B3LYP/6-31+G(d,p). Table S2: Selected geometric parameters and KS-MO energies for distorted Ph−P═P−Ph (B3LYP/6-311+G(2df,2p)). Figures S1, S2, and S3 showing comparisons of the ground state energy profile, KS-MO energies, and S_1-S_6 excited state energies, respectively, along the $\tau_1 = \tau_2$ coordinate for the two basis sets. Figure S1 also shows the ground state energy profile along the $\tau_1 = \tau_2$ diagonal for bis-(2,6-tBu$_2$C$_6$H$_2$) diphosphene. This material is available free of charge via the Internet at http://pubs.acs.org.

References and Notes

(1) Yoshifuji, M.; Shima, I.; Inamoto, N.; Hirotsu, K.; Higuchi, T. Synthesis and Structure of Bis(2,4,6-tri-tert-butylphenyl)diphosphene: Isolation of a True "Phosphobenzene". *J. Am. Chem. Soc.* **1981**, *103*, 4587–4589.

(2) Power, P. P. Homonuclear Multiple Bonding in Heavier Main Group Elements. *J. Chem. Soc., Dalton Trans.* **1998**, 2939–2951.

(3) Weber, L. The Chemistry of Diphosphenes and their Heavy Congeners: Synthesis, Structure, and Reactivity. *Chem. Rev.* **1992**, *92*, 1839–1906.

(4) Norman, N. C. Stable Compounds of the Heavier Group 14 and 15 Elements involving $p\pi$-$p\pi$ Multiple Bonding: An Overview of the First Decade. *Polyhedron* **1993**, *12* (20), 2431–2446.

(5) Power, P. P. π-Bonding and the Lone Pair Effect in Multiple Bonds between Heavier Main Group Elements. *Chem. Rev.* **1999**, *99*, 3463–3503.

(6) Yoshifuji, M. Sterically Protected Organophosphorus Compounds in Low Co-ordination States. *J. Chem. Soc., Dalton Trans.* **1998**, 3343–3349.

(7) Cowley, A. H. Stable Compounds with Double Bonding between the Heavier Main-Group Elements. *Acc. Chem. Res.* **1984**, *17*, 386–392.

(8) Cowley, A. H. Double Bonding between the Heavier Main-Group Elements: From Reactive Intermediates to Isolable Molecules. *Polyhedron* **1984**, *3* (4), 389–432.

(9) Liu, Z. F.; Hashimoto, K.; Fujishima, A. Photoelectrochemical information storage using an azobenzene derivative. *Nature* **1990**, *347*, 658–660.

(10) Zhang, C.; Du, M.-H.; Cheng, H.-P.; Zhang, Z.-G.; Roitberg, A. E.; Krause, J. L. Coherent Electron Transport through an Azobenzene Molecule: A Light-driven Molecular Switch. *Phys. Rev. Lett.* **2004**, *92* (15), 158301-1–158301-4.

(11) Balzani, V.; Credi, A.; Marchioni, F.; Stoddart, J. F. Artificial molecular-level machines. Dethreading-rethreading of a pseudorotaxane powered exclusively by light energy. *Chem. Commun.* **2001**, *2001*, 1860–1861.

(12) Banerjee, I. A.; Yu, L.; Matsui, H. Application of Host-Guest Chemistry in Nanotube-Based Device Fabrication: Photochemically Controlled Immobilization of Azobenzene Nanotubes on Patterned a-CD Monolayer/Au Substrates via Molecular Recognition. *J. Am. Chem. Soc.* **2003**, *125*, 9542–9543.

(13) Ikeda, T.; Tsutsumi, O. Optical Switching and Image Storage by Means of Azobenzene Liquid-Crystal Films. *Science* **1995**, *268*, 1873–1875.

(14) Tsutsumi, O.; Shiono, T.; Ikeda, T.; Galli, G. Photochemical Phase Transition Behavior of Nematic Liquid Crystals with Azobenzene Moieties as Both Mesogens and Photosensitive Chromophores. *J. Phys. Chem. B.* **1997**, *101*, 1332–1337.

(15) Meier, H. The Photochemistry of Stilbenoid Compounds and Their Role in Materials Technology. *Angew. Chem., Int. Ed. Engl.* **1992**, *31*, 1399–1420.

(16) Dainippon Ink and Chemicals, Inc., Kawamura Physical and Chemical Research Institute Portable Body Warmer. 1981 (Japan: JP 79-126436 19791002).

(17) For example: Adelman, A. H.; Nathan, R. A.; Schwerzel, R. E.; Wyant, R. E. A Process for solar energy collection and retrieval employing reversible photochemical isomerization. 1979 (Great Britain: GB 76-43557 19761020).

(18) Smith, R. C.; Protasiewicz, J. D. Systematic Investigation of PPV Analogue Oligomers Incorporating Low-Coordinate Phosphorus Centers. *Eur. J. Inorg. Chem.* **2004**, *2004*, 998–1006.

(19) Smith, R. C.; Protasiewicz, J. D. Conjugated Polymers Featuring Heavier Main Group Element Multiple Bonds: A Diphosphene-PPV. *J. Am. Chem. Soc.* **2004**, *126*, 2268–2269.

(20) Gates, D. P. Expanding the Analogy Between P═C and C═C Bonds to Polymer Science. *Top. Curr. Chem.* **2005**, *250*, 107–126.

(21) Baumgartner, T.; Reau, R. Orgaonphosphorus π-Conjugated Materials. *Chem. Rev.* **2006**, *106*, 4681–4727.

(22) Wang, Y.; Ma, J.; Jiang, Y. Tuning of Electronic Structures of Poly(*p*-phenylenevinylene) Analogues of Phenyl, Thienyl, Furyl, and Pyrrolyl by Double-Bond Linkages of Group 14 and 15 Elements. *J. Phys. Chem. A* **2005**, *109*, 7187–7206.

(23) Dutan, C.; Shah, S.; Smith, R. C.; Choua, S.; Berclaz, T.; Geoffroy, M.; Protasiewicz, J. D. Sterically Encumbered Diphosphaalkenes and a Bis(diphosphene) as Potential Multiredox-Active Molecular Switches: EPR and DFT Investigations. *Inorg. Chem.* **2003**, *42* (20), 6241–6251.

(24) Cowley, A. H.; Decken, A.; Norman, N. C.; Kruger, C.; Lutz, F.; Jacobsen, H.; Ziegler, T. Electron Density Distribution in Diphosphenes and the Nature of the Phosphorus-Phosphorus Double Bond: Experimental and Theoretical Studies. *J. Am. Chem. Soc.* **1997**, *119*, 3389–3390.

(25) Urzenius, E.; Protasiewicz, J. D. Synthesis and Structure of New Hindered Aryl Phosphorus Centers (Center = 2,6-Dimesitylphenyl). *Main Group Chem.* **1996**, *1* (4), 369–372.

(26) Frisch, M. J.; et al. *Gaussian 03 (Revision D.01)*; Gaussian, Inc.: Pittsburgh, PA, 2003.

(27) Becke, A. D., III. The role of exact exchange. *J. Chem. Phys.* **1993**, *98*, 5648–5652.

(28) Lee, C.; Yang, W.; Parr, R. G. Development of the Colle-Salvetti correlation-energy formula into a functional of the electron density. *Phys. Rev. B* **1988**, *37*, 785.

(29) Stephens, P. L.; Devlin, F. J.; Chabalowski, C. F.; Frisch, M. J. Ab Initio Calculation of Vibrational Absorption and Circular Dichroism Spectra Using density Functional Forces Field. *J. Phys. Chem.* **1994**, *98* (45), 11623.

(30) Petersson, G. A.; Al-Laham, M. A. *J. Chem. Phys.* **1991**, *94*, 6081.

(31) Sousa, S. F.; Fernandes, P. A.; Ramos, M. J. General Performance of Density Functionals. *J. Phys. Chem. A* **2007**, *111*, 10439–10452.

(32) Zhao, Y.; Truhlar, D. G. Density Functionals With Broad Applicability in Chemistry. *Acc. Chem. Res.* **2008**, *41* (2), 157–167.

(33) Hawforth, N. L.; Bacskay, G. B. Heats of formation of phosphorus compounds determined by current methods of computational quantum chemistry. *J. Chem. Phys.* **2002**, *117* (24), 11175–11187.

(34) Koch, W.; Holthausen, M. C. *A Chemist's Guide to Density Functional Theory*; WILEY-VCH Verlag: Weinheim, 2000.

(35) Stowasser, R.; Hoffmann, R. What Do the Kohn-Sham Orbitals and EigenValues Mean? *J. Am. Chem. Soc.* **1999**, *121*, 3414–3420.

(36) Shah, S.; Burdette, S. C.; Swavey, S.; Urbach, F. L.; Protasiewicz, J. D. Alkali Metal Induced Rupture of a Phosphorus-Phosphorus Double Bond. Electrochemical and EPR Investigations of New Sterically Protected Diphosphenes and Radical Anions $[ArPPAr]^{\bullet-}$. *Organometallics* **1997**, *16*, 3395–3400.

(37) Dennington, R., II; Keith, T.; Millam, J.; Eppinnett, K.; Hovell, W. L.; Gilliland, R. *GaussView, Version 3.09*; Semichem, Inc.: Shawnee Mission, KS, 2003.

(38) Kutzelnigg, W. Chemical Bonding in Higher Main Group Elements. *Angew. Chem., Int. Ed. Engl.* **1984**, *23*, 272–295.

(39) Amatatsu, Y. Theoretical Study on the Phenyl Torsional Potentials of *trans*-Diphenyldiphosphene. *J. Phys. Chem. A* **2008**, *112* (37), 8824–8828.

(40) With B3LYP/6-31+G(d,p), the central−P═P−unit is nearly planar (175.8°), the phenyl rings are twisted by 34°, and the C−P═P angle is 102.3°. The energy differences between the minimum and the maxima at 0° and 90° are 0.0324 eV (0.746 kcal/mol) and 0.195 eV (4.49 kcal/mol), respectively. See Supporting Information for a more detailed comparison.

(41) The study by Y. Amatatsu (ref 39) optimized geometries of Ph−P═P−Ph at the CASSCF level, and then calculated energies at using second-order multi-reference Møller-Plesset perturbation theory. The value for the barrier to phenyl rotation was not reported, however Figure 4a in that reference indicates a barrier of approximately 0.12 eV.

(42) Petsana, D. C.; Power, P. P. Synthesis and X-ray Structures of Compounds Having Very Short Phosphorus-Phosphorus Single Bonds: How Much of the Shortening in P-P Double Bonds is Due to p-p π Overlap? *J. Am. Chem. Soc.* **1989**, *111*, 6887–6888.

(43) Petsana, D. C.; Power, P. P. Synthesis and Structure of Diarylboryl-Substituted Hydrazines and Diphosphanes: Role of σ-Orbital Hybridization and π-Orbital Overlap in N-N and P-P Multiple-Bond Lengths. *Inorg. Chem.* **1991**, *30*, 528–535.

(44) Cotton, F. A.; Cowley, A. H.; Feng, X. The Use of Density Functional Theory To Understand and Predict Structures and Bonding in Main Group Compounds with Multiple Bonds. *J. Am. Chem. Soc.* **1998**, *120*, 1795–1799.

(45) The π-increment is that portion of the bond energy attributed to π-bonding; the σ-increment is the contribution of the σ-bonding to the bond energy.

(46) Galbraith, J. M.; Blank, E.; Shaik, S.; Hiberty, P. C. Pi-Bonding in Second and Third Row Molecules: Testing the Strength of Linus's Blanket. *Chem.−Eur. J.* **2000**, *6* (13), 2425–2434.

(47) Schoeller, W. W.; Bergemann, C.; Tubbesing, U.; Strutwolf, J. On the π-bond Strengths in Higher Element Homolougues of Methylenephosphane and Diphosphene. *J. Chem. Soc., Faraday Trans.* **1997**, *93* (17), 2957–2962.

(48) Miqueu, K.; Sotiropoulos, J.-M.; Pfister-Guillouzo, G.; Ranaivonjatovo, H.; Escudie, J. The electronic nature of the -Pn═Pn- Derivatives (Pn═P/As). New Insight, in the light of UV photoelectron spectroscopy. *J. Mol. Struct.* **2001**, *545*, 139–146.

(49) A DFT study of Ph−P═P−Ph using the B3PW91 functional (Cotton, F. A.; Cowley, A. H.; Feng, X. *J. Am. Chem. Soc.* **1998**, *120*, 1795–1799.) also found that the HOMO was a σ orbital, however the phenyl twist angle was not reported.

(50) Lee, J.-G.; Cowley, A. H.; Boggs, J. E. Theoretical Modeling of the Diphosphene (HP═PH) Ligand. *Inorg. Chim. Acta* **1983**, *77*, L61-L62.

(51) Cetinkaya, B.; Lappart, M. F.; Stamper, J. G.; Suffolk, R. J. The He(I) and He(II) Photoelectron spectra of bis (2,4,6-tri-*t*-butylphenyl)-diphosphene. *J. Electron Spectrosc. Relat. Phenom.* **1983**, *32*, 133–137.

(52) Nagase, S.; Suzuki, S.; Kurakake, T. Do Distibene (HSb═SbH) and Dibismuthene (HBi═BiH) feature Double Bonding? A Theoretical Comparison with Diphosphene (HP═PH) and Diarsene (HAs═AsH). *J. Chem. Soc., Chem. Commun.* **1990**, *1990*, 1724–1726.

(53) Mahe, L.; Barthelat, J.-C. Is Phosphorus Able to form Double Bonds with Arsenic, Antimony, or Bismuth? An *ab initio* Study of the PXH2 Potential Energy Surfaces. *J. Phys. Chem.* **1995**, *99*, 6819–6827.

(54) Gonbeau, D.; Pfister-Guillouzo, G.; Escudie, J.; Couret, C.; Satge, J. Application de la Spectroscopie Moleculaire aux Proprietes Molecularires XVII*. Etude Structurale de Diphosphenes par Spectroscopie Photoelectronique. *J. Organomet. Chem.* **1983**, *247*, C17-C20.

(55) Galasso, V. Ab Initio Theoretical Study of Photoelectron and NMR Properties of Diazene, Phosphazene, Diphosphene, and Diarsene. *Chem. Phys.* **1984**, *83*, 407–413.

(56) Gonbeau, D.; Pfister-Guillouzo, G. Applications of Photoelectron Spectroscopy to Molecular Properties. XVIII. The Vertical Ionization Potentials of Diphosphene as Calculated by Perturbation Corrections to Koopmans' Theorem. *J. Electron Spectrosc. Relat. Phenom.* **1984**, *33*, 279–283.

(57) Gleiter, R.; Friedrich, G.; Yoshifuji, M.; Shibayama, K.; Inamoto, N. Photoelectron Spectra of Diaryldiphosphenes. *Chem. Lett.* **1984**, *1984*, 313–316.

(58) Allen, T. L.; Scheiner, A. C.; Yamaguchi, Y.; Schaefer, H. F., III. Theoretical Studies of Diphosphene and Diphosphinylidene in their Closed Shell States, Low-Lying Open-Shell Singlet and Triplet States, and Transition States. Search for a Stable Bridged Structure. *J. Am. Chem. Soc.* **1986**, *108*, 7579–7588.

(59) See Table 2 footnotes for abbreviations.

(60) In this notation, the ground electronic state has the configuration $(n_+^2\pi^{*0})$.

(61) The numbering scheme is modified from that of Klessinger and Michl *Excited States and Photochemistry of Organic Molecules* (1995) to include symmetry designations in the C_{2h} point group. Occupied KS-MOs are numbered from 1 to 56, beginning with the HOMO and moving downward in energy. Unoccupied KS-MOs are numbered from 1′ to 56′, beginning with the LUMO and moving upward. An excitation from the HOMO to the LUMO thus becomes a $1 \rightarrow 1'$ excitation, regardless of the nature of the KS-MOs involved.

(62) Shah, S.; Simpson, M. C.; Smith, R. C.; Protasiewicz, J. D. Three Different Fates for Phosphinidenes Generated by Photocleavage of Phospha-Wittig Reagents $ArP{=}PMe_3$. *J. Am. Chem. Soc.* **2001**, *123*, 6925–6926.

(63) Yoshifuji, M.; Sato, T.; Inamoto, N. Wavelength- and Temperature-dependent Photolysis of a Diphosphene. Generation of 2,4,6-tri-t-butylphenylphosphinidine and E/Z Isomerization. *Chem. Lett.* **1988**, 1735–1738.

(64) Peng, H.-L.; Payton, J. L.; Protasiewicz, J. D.; Simpson, M. C. First Observation of Diphosphene Excited States. Ultrafast Transient Absorption Spectroscopy. *J. Am. Chem. Soc.*, in preparation.

(65) Peng, H.-L. *Computational and Spectroscopic Studies of the Photochemistry and Photophysics of Diphosphenes*; Case Western Reserve University: Cleveland, 2007.

(66) Yoshifuji, M.; Sato, T.; Inamoto, N. Photoreaction of (E)-1-Mesityl-2-(2,4,6-tri-t-butylphenyl)diphosphene. *Bull. Chem. Soc. Jpn.* **1989**, *62*, 2394–2395.

(67) Yoshifuji, M.; Hashida, T.; Inamoto, N.; Hirotsu, K.; Horiuchi, T.; Higuchi, T.; Ito, K.; Nagase, S. E→Z Photoisomerization of a Diphosphene on Carbonylmetal Complexes (M═Cr, Mo, W). *Angew. Chem., Int. Ed. Engl.* **1985**, *24* (3), 211–212.

(68) Ito, S.; Nishide, D.; Yoshifuji, M. Synthesis of pentacarbonyltungsten(0) complexes of bulky 1,2-diphosphabut-1-en-3-ynes as a heavier enyne congener. *Tetrahedron Lett.* **2002**, *43*, 5075–5078.

(69) Yoshifuji, M.; Abe, M.; Toyota, K.; Goto, K.; Inamoto, T. Photochemical Reactions of Diphosphenes Carrying 2,4,6-Tris(trifluoromethyl)phenyl Group. *Bull. Chem. Soc. Jpn.* **1993**, *66*, 1572–1575.

(70) Komen, C. M. D.; de Kanter, F. J. J.; Goede, S. J.; Bickelhaupt, F. Synthesis, Photochemical Behavior and cis/trans Isomerization of 1-(2,4,6-triisopropylphenyl)-2-(2,4,6-tri-tert-butylphenyl)diphosphene. *J. Chem. Soc., Perkin Trans. 2* **1993**, 807–812.

(71) Riviere, F.; Ito, S.; Yoshifuji, M. Preparation and reaction of sterically crowded *N*-(2,4-di-*t*-butylphenyl)-*N*-methylaminodichlorophosphine. *Tetrahedron Lett.* **2002**, *43*, 119–121.

(72) Caminade, A.-M.; Verrier, M.; Ades, C.; Paillous, N.; Koenig, M. Laser Irradiation of a Diphosphene: Evidence for the First cis-trans Isomerization. *J. Chem. Soc., Chem. Commun.* **1984**, 875–877.

(73) Niecke, E.; Altmeyer, O.; Nieger, M. Synthesis, Structure, and Isomerization of the (E)- and (Z)- Isomers of a Diphosphene. *Angew. Chem., Int. Ed. Engl.* **1991**, *30* (9), 1136–1138.

(74) Jutzi, P.; Meyer, U. Photochemie von pentamethylcyclopentadienyl-substituierten Diphosphenen und Phosphaarsenen. *J. Organomet. Chem.* **1987**, *333*, C18-C20.

(75) Pietschnig, R.; Niecke, E. Synthesis, Spectroscopic Properties, and Reactivity of Ferrocenyl(2,4,6-tri-*tert*-butylphenyl)diphosphene. *Organometallics* **1996**, *15*, 891–893.

(76) Niecke, E.; Kramer, B.; Nieger, M. Synthesis, Structure and Reactivity of Diphosphenes having a cis-Configuration. *Angew. Chem., Int. Ed. Engl.* **1989**, *28* (2), 215–217.

(77) Schultz, T.; Quenneville, J.; Levine, B.; Toniolo, A.; Martinez, T. J.; Lochbrunner, S.; Schmitt, M.; Shaffer, J. P.; Zgierski, M. Z.; Stolow, A. Mechanism and Dynamics of Azobenzene Photoisomerization. *J. Am. Chem. Soc.* **2003**, *125*, 8098–8099.

(78) Sasamori, T.; Takeda, N.; Tokitoh, N. Synthesis and reactions of new diphosphenes bearing extremely bulky substituents. *J. Phys. Org. Chem.* **2003**, *16*, 450–462.

(79) Toyota, K.; Kawasaki, S.; Nakamura, A.; Yoshifuji, M. Preparation and Properties of Sterically Protected Diphosphene and Fluorenylidenephosphine Bearing the 2,6-Di-*tert*-butyl-4-methoxyphenyl Group. *Chem. Lett.* **2003**, *32* (5), 430–431.

(80) Kawasaki, S.; Nakamura, A.; Toyota, K.; Yoshifuji, M. The Electronic Effects of Bulky Aryl Substituents on Low Coordinated Phosphorus Atoms in Diphosphenes and Phosphaalkenes by Functionalization at the Para Position. *Bull. Chem. Soc. Jpn.* **2005**, *78*, 1110–1120.

(81) Smith, R. C.; Ren, T.; Protasiewicz, J. D. A Robust, Reactive, and Remarkably Simple to Prepare Stericaly Encumbered *meta*-Terphenyl Ligand. *Eur. J. Inorg. Chem.* **2002**, *2002* (11), 2779–2783.

(82) Escudie, J.; Couret, C.; Ranaivonjatovo, H.; Lazraq, M.; Satge, J. Synthesis of two stable diphosphenes with a new stabilizing substituent. *Phosphorus Sulfur Relat. Elem.* **1987**, *31*, 27–31.

(83) Dubourg, A.; Declerq, J. P.; Ranaivonjatovo, H.; Escudie, J.; Couret, C.; Lazraq, M. Structure of Bis[2,6-bis(trifluoromethyl)phenyl]diphosphene. *Acta Cryst.* **1988**, *C44*, 2004–2006.

JP810119K